Journal of Energy Storage 15 (2018) 329–335

Contents lists available at ScienceDirect

Journal of Energy Storage

journal homepage: www.elsevier.com/locate/est

Electrochemical performance of Mo doped high voltage spinel cathode material for lithium-ion battery

T. Kazda[a,*], J. Vondrák[a], A. Visintin[b], M. Sedlaříková[a], J. Tichý[a], P. Čudek[a]

[a] Department of Electrical and Electronic Technology, Faculty of Electrical Engineering and Communication, Brno University of Technology, Technická 10, 616 00, Brno, Czech Republic
[b] Instituto de Investigaciones Fisicoquímicas Teóricas y Aplicadas (INIFTA), UNLP, CCT La Plata-CONICET, CC 16, Suc. 4, CP 1900, La Plata, Argentina

ARTICLE INFO

Article history:
Received 15 September 2017
Received in revised form 17 October 2017
Accepted 17 October 2017
Available online xxx

Keywords:
Lithium ion battery
High voltage cathode material
Solid-state reactions
Mo doping

ABSTRACT

This article deals with the properties of high-voltage cathode material $LiNi_{0.5}Mn_{1.5}O_4$ synthesized by a solid-state reaction method and the influence of doping this material by molybdenum. The samples – $LiMo_{x+y}Ni_{0.5-x}Mn_{1.5-y}O_4$ with different Mo contents ($x = 0.00, 0.05$, $y = 0.00, 0.05$) were successfully synthesized by two step annealing process and they were then investigated by SEM, EDS spectroscopy, thermo gravimetric analysis, cyclic voltammetry and charge–discharge tests at different loads and high temperature in lithium-ion cells with metal lithium as a counter electrode. Results showed that the initial discharge capacity and capacity during high temperature cycling of the $LiMo_{x+y}Ni_{0.5-x}Mn_{1.5-y}O_4$ cathode were improved with addition of Mo when x = 0.05. Thermal analysis results suggested that the Mo doping slightly improved the stability of the crystal structure of the $LiNi_{0.5}Mn_{1.5}O_4$ cathode which leads to an improved stability during high temperature galvanostatic cycling.

1. Introduction

Researchers focused their interest toward modifications of existing cathode materials in order to improve their parameters as a result of searching for new types of cathode materials which could replace currently used cathode materials and allow resolving problems related to the requirements of increasingly higher demand for electrical energy storage particularly in the field of electric vehicles. The result of one of those efforts was the discovery of the cathode material $LiNi_{0.5}Mn_{1.5}O_4$ [1–3]. This material is based on the cathode material $LiMn_2O_4$ in which manganese was partially replaced by nickel. This replacement makes possible charging of the cathode material to 5 V [2,4]. $LiNi_{0.5}Mn_{1.5}O_4$ spinel is same like $LiMn_2O_4$. There are two kinds of crystalline structures depending on the method of synthesis of this material: face centered cubic (Fd3m), referred in the literature as disordered and simple cubic ($P4_332$), referred in the literature as ordered [4–6]. The $LiNi_{0.5}Mn_{1.5}O_4$ material suffers with the same problem as $LiMn_2O_4$- dissolution of manganese into the electrolyte during cycling at higher temperatures which leads to defects in the structure and capacity decrease [4,7–9]. If we take into account the high theoretical capacity of this material (148 mAh/g) and its high potential against lithium (~4.7 V) we get the gravimetric energy density approaching 700 Wh/kg which is approximately 20% more than gravimetric energy density of $LiCoO_2$ and about 30% more than in the case of the cathode material $LiFePO_4$ [8,10]. This cathode material is stable during long term cycling and exhibits good stability at higher current loads because of the spinel structure. These properties make this material interesting for example for use in electric vehicles. This cathode material reaches the high voltage using several oxidation steps at which there occur conversions $LiNi_{0.5}^{II}Mn_{1.5}^{III}O_4/Ni_{0.5}^{IV}Mn_{1.5}^{IV}O_4$. Mn^{3+} oxidizes to Mn^{4+} at 4 V vs Li and Ni^{2+} is subsequently oxidized to Ni^{3+} at the voltage range 4.7–4.8 V vs Li and then to Ni^{4+}. The result of these successive changes of valence of nickel is merging of two discharge plateaus in one very stable discharge plateau [2,4,5,11]. There is the possibility of doping of $LiNi_{0.5}Mn_{1.5}O_4$ with other of other metals to solve the problem of this material with instability at high temperatures. Several different materials were already used for doping, e.g. copper. The amount of doped Cu affects the lattice parameter, lattice configuration, morphology of particles and electrochemical properties. The added copper participates in the electrochemical reaction during charging/discharging thanks to the change in valence of Cu^{+2} to Cu^{+3} [4,12]. The reversible capacity decreases with the increasing amount of Cu but proper optimization of the ratio can improve stability at high loads. E.g. the

* Corresponding author.
E-mail address: kazda@feec.vutbr.cz (T. Kazda).

https://doi.org/10.1016/j.est.2017.10.011
2352-152X/

material $LiCu_{0,25}Ni_{0,25}Mn_{1,5}O_4$ is due to doping more conductive and the electrochemical properties of this material are consequently enhanced [4]. Another option that has been tested was doping by ruthenium. The materials $LiNi_{0.5}Mn_{1.5}O_4$, $Li_{1.1}Ni_{0.35}Ru_{0.05}Mn_{1.5}O_4$ and $LiNi_{0.4}Ru_{0.05}Mn_{1.5}O_4$ were compared. It has been found, by EIS measurement, that the conductivity rises which leads to the increase of capacity despite of a small part of the active Ni being replaced by Ru [13]. Doping by Cr was also tested, a partial replacement of Ni by Cr occurred in this case. The ionic radius of Cr^{+3} is 0.615 Å which is close to the ion radius of Ni^{+2} (0.65 Å). Partial substitution, such as $LiNi_{0.45}Cr_{0.05}Mn_{1.5}O_4$, leads to improved electrochemical properties due to higher bond strength of the Cr—O bond than in the case of the bonds Ni—O and Mn—O. The stronger Cr—O bond leads to an increase of the rigidity of the material structure and maintaining the properties during long term cycling at higher loads and higher temperatures. Another advantage is that chromium participates in the reaction and the change of valence of Cr^{+3} to Cr^{+4} and back takes place during cycling which leads to the shift of potential of the discharging plateau to 4.8 V against Li [14–16]. A similar phenomenon also occurs during the doping of the material by Al. The ionic radius of Al^{3+} is 0.62 Å and similarly the capacity during cycling at higher loads is stable thanks to the strong Al—O bond [17]. Other elements that have been studied with the aim to improve the properties of the material $LiNi_{0.5}Mn_{1.5}O_4$ were e.g. Fe [18], Co [19], Ti [20], Mg [21], Rh [22] and W [23] .

2. Experimental

The method of reaction in solid state was chosen for the production of this material. Precursors based on carbonates and oxides were chosen as basic materials for the production. Li_2CO_3 (Lithium(II) carbonate), $MnCO_3$ (Manganese carbonate), NiO (Nickel oxide) and MoO_2 (Molybdenum(IV) oxide) were chosen in our case; these materials were mixed in a stechiometric ratio of 0.02 mol/l. The two-step annealing process was selected for the preparation. Selected precursors are milled together in the ball mill FRITSCH Pulverisette 0 for 4 h during the first step of this process. In the first annealing step, the resultant mixture is annealed at 600 °C for 10 h. The second step is annealing at 900 °C for 15 h [24]. After this synthesis, we obtain materials with face-centered spinel structure therefore known as disordered. The prepared material was then mixed into a mixture consisting of NMP (*N*-Methyl-2-pyrrolidon) (solvent), PVDF (Polyvinylidenfluorid) (binder) and carbon Super P. The weight ratio of the materials was: active material 80%, Super P 10%, PVDF 10%. The resulting mixture was subsequently deposited on an Al foil, dried and pressed by the pressure of 3200 kg/cm^2. A disk with a diameter of 18 mm was cut out of the coated aluminium foil and inserted into the electrochemical test cell El-Cell© ECC-STD. The assembly was done in a glove box filled with argon atmosphere. Metal Lithium was used as a material for the anode and electrolyte was soaked in a glass fibre separator. 1.5 mol/l $LiPF_6$ EC:DMC 1:2 *w/w* was used as electrolyte.

Cyclic voltammetry and galvanostatic cycling were used for electrochemical characterisation. Cyclic voltammetry was done in the potential window from 3.0 to 5.1 V versus lithium and the scan rate was set to 0.5 mV/s. Galvanostatic cycling was carried out with the same potential window from 3.0 to 5.1 V versus lithium. Two charging and discharging cycles were carried out each time during which the used charging and discharging currents were set to 60 mA/g (related to the weight of the active mass). The real capacity value of the sample was deducted from these two cycles and the sample was then exposed to long term cycling during which it was cycled twenty times by 0.5C current. It was subsequently cycled five times by 1C current, then five times by 2C and then five times by 5C. The next step was cycling again five times by 2C current, again five times by 1C, again ten times by 0.5C and finally there were ten cycles by 0.5C current at the temperature of 50 °C. An assembly consisting of a SEM microscope TESCAN VEGA3 XMU and a Bruker EDAX analyser was used to determine the distribution of elements in the materials. TGA (Thermogravimetric analysis) was used for comparison of thermal stability of the doped cathode materials.

3. Results and discussion

We can see the structure of the samples $LiNi_{0.5}Mn_{1.5}O_4$, $LiMo_{0.05}Ni_{0.45}Mn_{1.5}O_4$ and $LiMo_{0.1}Ni_{0.45}Mn_{1.45}O_4$ after synthesis displayed by SEM in Fig. 1. We can see the structure of the cathode material $LiNi_{0.5}Mn_{1.5}O_4$ after synthesis in Fig. 1A). Used field of view is the same as for other SEM Pictures – 20.8 μm. As we can see there are aggregates of small crystals in the entire volume. The size of the crystals is smaller than 5 μm. SEM analysis of the $LiMo_{0.05}Ni_{0.45}Mn_{1.5}O_4$ cathode material sample is displayed in Fig. 1B). It is clearly evident from the figure that the crystals are interconnected and their size is comparable with the size of crystals of the pristine cathode material $LiNi_{0.5}Mn_{1.5}O_4$. We can see SEM picture of the cathode material $LiMo_{0.1}Ni_{0.45}Mn_{1.45}O_4$ in Fig. 1C); the structure is, in comparison with the two previous samples, different and facets of the crystals are not clearly visible. However, the size of separate particles is approximately similar as the size of particles in the two previous samples (less than 5 μm).

EDS (Energy-dispersive X-ray spectroscopy) analysis with surface mapping of the sample was performed together with the SEM analysis. The EDS spectrum of the samples $LiNi_{0.5}Mn_{1.5}O_4$, $LiMo_{0.05}Ni_{0.45}Mn_{1.5}O_4$ can be seen in Fig. 2. We can see the EDS spectrum obtained from a sample of the cathode material $LiNi_{0.5}Mn_{1.5}O_4$ in Fig. 2A). It is evident from the recorded spectra that the material contains all estimated elements (Ni, Mn, and O). The EDS spectrum obtained from a sample of the cathode material

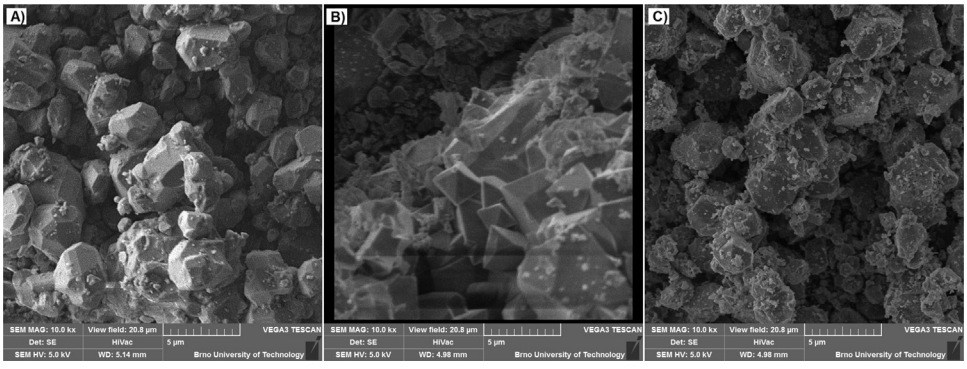

Fig. 1. SEM analysis of the samples A) $LiNi_{0.5}Mn_{1.5}O_4$, B) $LiMo_{0.05}Ni_{0.45}Mn_{1.5}O_4$ and C) $LiMo_{0.1}Ni_{0.45}Mn_{1.45}O_4$; used view field: 20.8 μm.

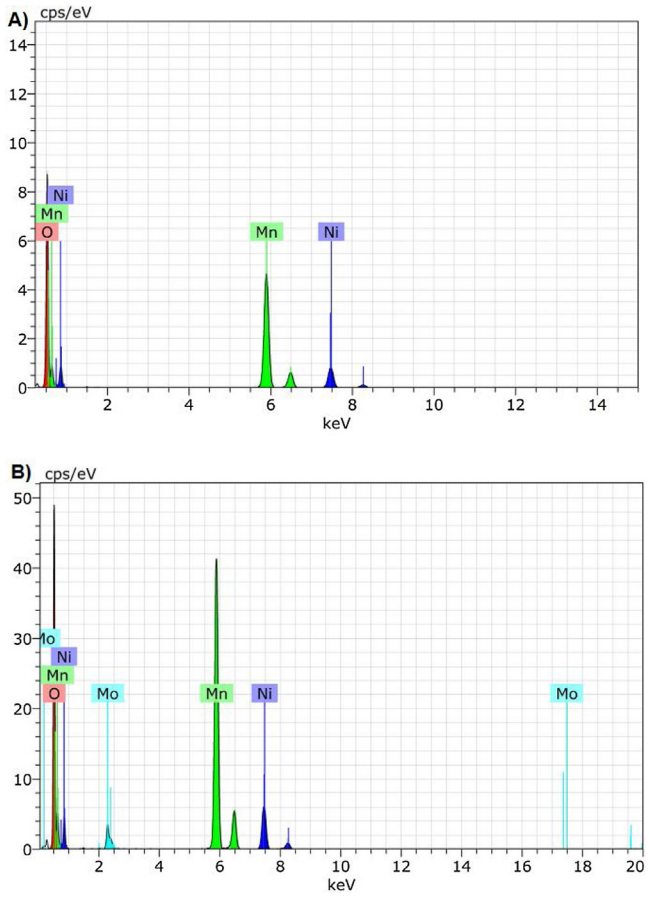

Fig. 2. EDS analysis of the sample A) $LiNi_{0.5}Mn_{1.5}O_4$, B) $LiMo_{0.05}Ni_{0.45}Mn_{1.5}O_4$.

$LiMo_{0.05}Ni_{0.45}Mn_{1.5}O_4$ is displayed in Fig. 2B). Again, we can see that the spectrum contains all the peaks corresponding to the required elements (Ni, Mn, Mo, and O). The map of distribution of each element is shown in Fig. 3. Fig. 31) confirms the demanded uniformity of the distribution of Mn, Ni and O in the investigated material $LiNi_{0.5}Mn_{1.5}O_4$.

The synthesized cathode materials $LiNi_{0.5}Mn_{1.5}O_4$, $LiMo_{0.05}Ni_{0.45}Mn_{1.5}O_4$ and $LiMo_{0.1}Ni_{0.45}Mn_{1.45}O_4$ was also analyzed by TG to investigate its thermal stability. This analysis was done in air and the range of temperatures was from room temperature to 900 °C. The heating rate was 10 °C/min. The result of this analysis is in Fig. 4 and from the chart we can assume all the materials are very stable and there was no significant loss of weight up to 600 °C. The specimen also does not contain any water or carbon residuals, which could remain there after the synthesis. However, some differences are evident in a closer comparison between the samples. The most stable one is the cathode material $LiMo_{0.05}Ni_{0.45}Mn_{1.5}O_4$ which is very stable up to the temperature exceeding 600 °C without any decline and after this stable area there is subsequently a sharp drop of weight. We can see a slight decrease of weight at about 400 °C and a high weight decrease after exceeding 600 °C for the sample of the pristine cathode material $LiNi_{0.5}Mn_{1.5}O_4$ similarly as for the previous sample but now the drop is sharper. The least stable sample is the cathode material $LiMo_{0.1}Ni_{0.45}Mn_{1.45}O_4$ which weight at about 400 °C also decreased but more significantly than in the case of pristine cathode material and the decrease above 600 °C is higher in this case. The weight decrease above 600 °C is typical for this high-voltage cathode material and it is caused by losing oxygen and lithium from the cathode structure [14,25]. It was successfully confirmed that the addition of small amounts of chromium leads to strengthening of the structure and this decline from 600 °C is not too sharp [14]. A similar improvement of the structure strength probably occurred for the $LiMo_{0.05}Ni_{0.45}Mn_{1.5}O_4$ sample.

Voltammogram of all samples obtained during CV at the scan rate 0.5 mV/s is shown in Fig. 5. We can see that all molybdenum doped samples increased their activity in the area around 4 V. Which is the area where the changes in valence of manganese from Mn^{3+} to Mn^{4+} and back occur. It can be concluded from this that the addition of Mo leads to the fact that a greater amount of Mn in the sample remains in the Mn^{3+} state after the synthesis. This activity around 4 V is higher for the sample $LiMo_{0.05}Ni_{0.45}Mn_{1.5}O_4$ than in the case of the sample $LiMo_{0.1}Ni_{0.45}Mn_{1.45}O_4$ which is probably caused by reducing the total amount of Mn in the material to the detriment of an increased amount of Mo. When we compare the anodic side of the peak in the high potential range over 4.6 V we can see that pure cathode material $LiNi_{0.5}Mn_{1.5}O_4$ has two

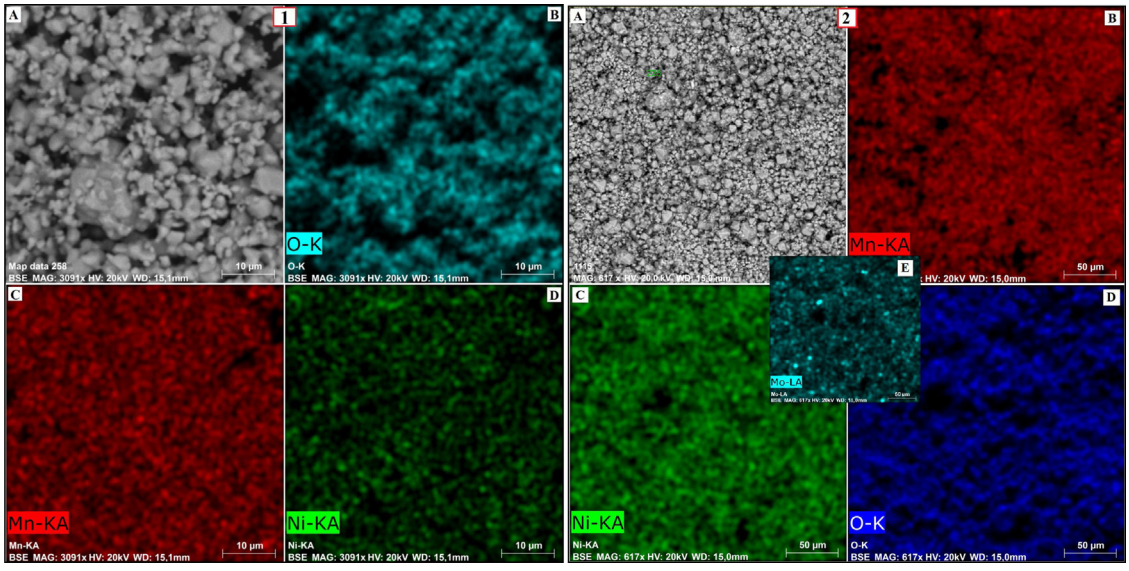

Fig. 3. Mapping of the sample of 1) $LiNi_{0.5}Mn_{1.5}O_4$ A) SEM particles $LiNi_{0.5}Mn_{1.5}O_4$ B) distribution of oxygen C) distribution of manganese D) distribution of nickel 2) $LiMo_{0.05}Ni_{0.45}Mn_{1.5}O_4$ A) SEM particles $LiMo_{0.05}Ni_{0.45}Mn_{1.5}O_4$ B) distribution of manganese C) distribution of nickel D) distribution of oxygen E) distribution of molybdenum.

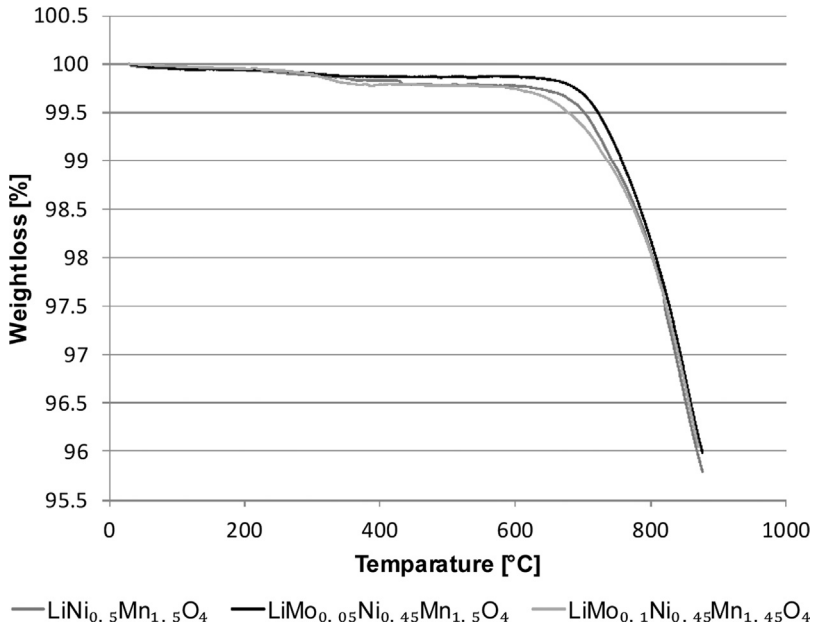

Fig. 4. TGA analysis of the samples $LiNi_{0.5}Mn_{1.5}O_4$, $LiMo_{0.05}Ni_{0.45}Mn_{1.5}O_4$ and $LiMo_{0.1}Ni_{0.45}Mn_{1.45}O_4$.

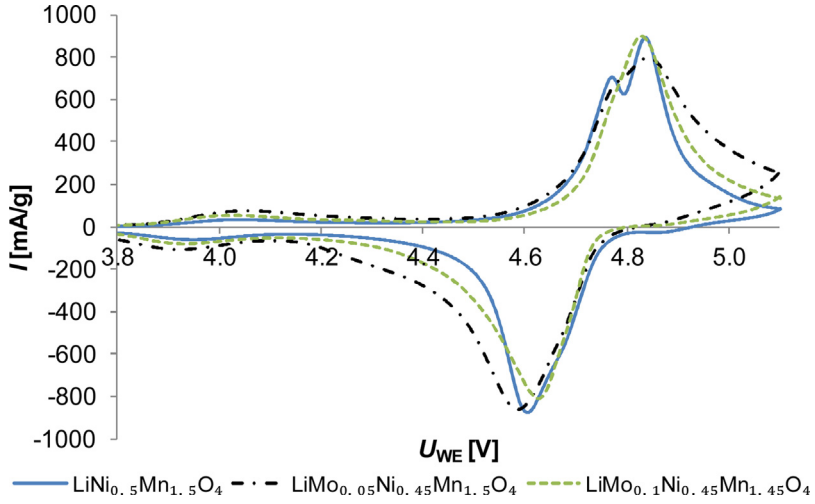

Fig. 5. Comparison of CV of the samples $LiNi_{0.5}Mn_{1.5}O_4$, $LiMo_{0.05}Ni_{0.45}Mn_{1.5}O_4$ and $LiMo_{0.1}Ni_{0.45}Mn_{1.45}O_4$; scan rate of 0.5 mV/s.

consecutive oxidation peaks and the cathode material $LiMo_{0.05}Ni_{0.45}Mn_{1.5}O_4$ has these two peaks as well but they are closer to each other and almost coincide. It is then evident in the case of the material with the highest proportion of Mo that these peaks merged and only one oxidation peak was created. It follows from these results that with increasing amounts of Mo in the structure the potentials related to the change of valence of nickel Ni^{2+} to Ni^{3+} and subsequently to Ni^{4+} approach each other. We can see on the side of cathodic peaks at higher potential that the activity increase of Mo doped samples occurs at a slightly lower potential than in the case of pure cathode material $LiNi_{0.5}Mn_{1.5}O_4$.

Fig. 6 shows discharge capacities achieved during the whole cycling by different loads and also the influence of higher temperature for all samples. The measurement was started by cycling by 0.5C (20 cycles). The highest observed capacity had the sample $LiMo_{0.05}Ni_{0.45}Mn_{1.5}O_4$ which reached 125.3 mAh/g in the first cycle. However, this capacity decreased during twenty cycles to 115.1 mAh/g. As we can see, the most stable sample was the pristine $LiNi_{0.5}Mn_{1.5}O_4$ for which the capacity decreased from 115.4 mAh/g to 113.3 mAh/g. The least stable sample during first twenty cycles was $LiMo_{0.1}Ni_{0.45}Mn_{1.45}O_4$. This sample was also the most unstable among all samples during cycling at higher C-rates. If we compare capacity of the pristine sample $LiNi_{0.5}Mn_{1.5}O_4$ and the sample $LiMo_{0.05}Ni_{0.45}Mn_{1.5}O_4$ at higher C-rates we can see that they are almost the same and during reducing of the load down to 1C they come back to their previous capacities. We can see that sample $LiMo_{0.05}Ni_{0.45}Mn_{1.5}O_4$ reached higher capacity 112.1 mAh/g after returning to the initial load of 0.5C (approximately 2.6% less than in the last cycle in previous cycling at 0.5C) than the pristine sample $LiNi_{0.5}Mn_{1.5}O_4$ – 107.5 mAh/g (approximately 5.1% less than in the last cycle in previous cycling at 0.5C). An increase of capacity occurred during cycling at high temperature for all samples (due to the higher mobility of particles at higher temperature) but this capacity soon rapidly decreased. The most stable sample during these ten cycles at 0.5C at high temperature was $LiMo_{0.05}Ni_{0.45}Mn_{1.5}O_4$. It lost 4.1% of its capacity which is much less than 19.6% of capacity which was lost by the pristine sample $LiNi_{0.5}Mn_{1.5}O_4$. The overall decrease of capacity during the whole

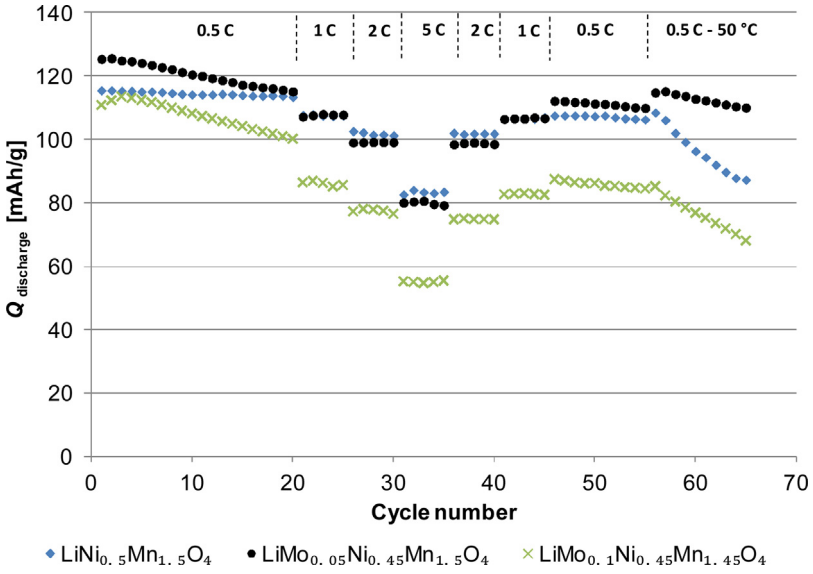

Fig. 6. Comparison of change of capacity of the sample $LiNi_{0.5}Mn_{1.5}O_4$, $LiMo_{0.05}Ni_{0.45}Mn_{1.5}O_4$ and $LiMo_{0.1}Ni_{0.45}Mn_{1.45}O_4$ for different C-rate and temperature.

Table 1
Capacities and capacity decrease at different C-rates during cycling of all tested samples.

Sample – $LiNi_{0.5}Mn_{1.5}O_4$									
C – rates	0.5C		1C	2C	5C	2C	1C	0.5C	0.5C at 50 °C
Cycle number	1	20	21	26	31	36	41	46	65
Capacity [mAh/g]	115.4	113.3	107.6	102.5	82.6	102.0	106.3	107.5	87.2
Capacity decrease vs. 1st cycle		−1.8%	−6.8%	−11.2%	−28.4%	−11.6%	−7.9%	−6.8%	−24.4%
Capacity decrease vs. 20th cycle			−5.0%	−9.5%	−27.1%	−10.0%	−6.2%	−5.1%	−23.0%
Sample – $LiMo_{0.05}Ni_{0.45}Mn_{1.5}O_4$									
C – rates	0.5C		1C	2C	5C	2C	1C	0.5C	0.5C at 50 °C
Cycle number	1	20	21	26	31	36	41	46	65
Capacity [mAh/g]	125.3	115.1	107.1	99.0	80.0	98.4	106.4	112.1	110.0
Capacity decrease vs. 1st cycle		−8.2%	−14.5%	−21.0%	−36.2%	−21.5%	−15.1%	−10.6%	−12.2%
Capacity decrease vs. 20th cycle			−6.9%	−14.0%	−30.5%	−14.5%	−7.5%	−2.6%	−4.4%
Sample – $LiMo_{0.1}Ni_{0.45}Mn_{1.45}O_4$									
C – rates	0.5C		1C	2C	5C	2C	1C	0.5C	0.5C at 50 °C
Cycle number	1	20	21	26	31	36	41	46	65
Capacity [mAh/g]	110.8	100.1	86.4	77.2	55.1	74.7	82.6	87.4	68.0
Capacity decrease vs. 1st cycle		−9.7%	−22.0%	−30.3%	−50.3%	−32.6%	−25.5%	−21.1%	−38.6%
Capacity decrease vs. 20th cycle			−13.7%	−22.9%	−45.0%	−25.4%	−17.5%	−12.7%	−32.1%

cycling was 24.4% for the pristine sample $LiNi_{0.5}Mn_{1.5}O_4$, 12.3% for the sample $LiMo_{0.05}Ni_{0.45}Mn_{1.5}O_4$ and 38.6% for the sample $LiMo_{0.1}Ni_{0.45}Mn_{1.45}O_4$. The comparison of capacities and perceptual capacity decrease are shown in Table 1.

When we compare these results with the results that are presented in the article by Yi [26] which is so far the only one who synthesized Mo doped cathode material $LiNi_{0.5}Mn_{1.5}O_4$ (but by the sol-gel method) we find that he compared the Mo-doped materials with a very poor sample of the pristine material $LiNi_{0.5}Mn_{1.5}O_4$ which at the load of 2C reached the capacity of 68.5 mAh/g (charge rate 0.1C) which is lower than the capacity achieved by the pristine material $LiNi_{0.5}Mn_{1.5}O_4$ at 5C in this article – 82.6 mAh/g (with symmetrical charge/discharge current). In the case of doped samples, his sample $LiMn_{1.425}Ni_{0.5}Mo_{0.05}O_4$ reached the capacity of 107.4 mAh/g at 2C load which is comparable to the capacities which were reached by the sample $LiMo_{0.05}Ni_{0.45}Mn_{1.5}O_4$ presented in this article. His sample $LiMn_{1.4}Ni_{0.55}Mo_{0.05}O_4$ reached the capacity of 122.7 mAh/g which is indeed higher capacity but it was achieved at the charging current 0.1C.

There is the comparison of the first discharge curves for each sample in Fig. 7. It can be seen that all samples maintain very stable discharging plateau around 4.7 V. However, the discharge plateau of Mo doped samples is slightly lower which corresponds with the activity at lower cathode potential observed by CV. Capacity reached in the upper discharge plateau around 4.7 V is in the case of the sample $LiMo_{0.05}Ni_{0.45}Mn_{1.5}O_4$ comparable with the pristine sample $LiNi_{0.5}Mn_{1.5}O_4$ but Mo doped sample $LiMo_{0.05}Ni_{0.45}Mn_{1.5}O_4$ achieved higher overall capacity thanks to the higher 4 V discharge plateau which also corresponds with the data from CV which showed higher activity around 4 V in the case of Mo doped samples.

Fig. 8 shows the comparison of the last discharge curves during cycling at 2C for each sample. As we can see, capacities of pristine sample $LiNi_{0.5}Mn_{1.5}O_4$ and Mo-doped sample $LiMo_{0.05}Ni_{0.45}Mn_{1.5}O_4$ are almost the same and both samples maintain their potential of high-voltage discharge plateau at almost the same level as during the discharge by 0.5C current. The sample $LiMo_{0.1}Ni_{0.45}Mn_{1.45}O_4$ reached much lower capacity and also the

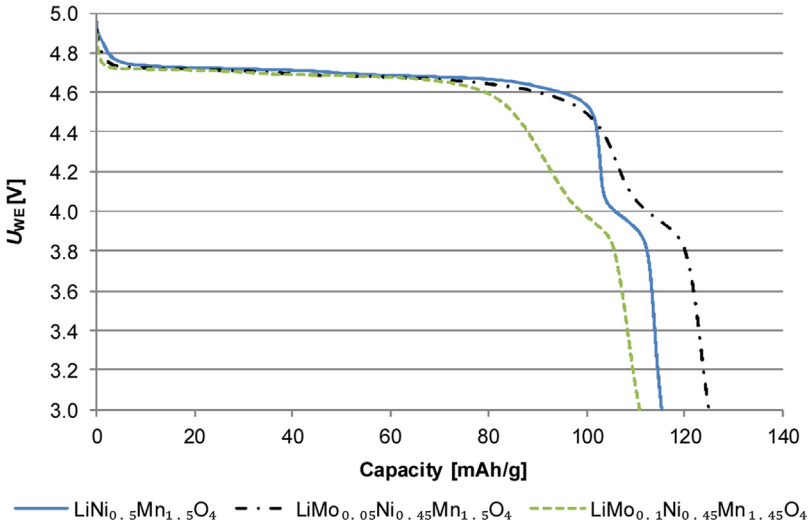

Fig. 7. Comparison of the first discharge curves of the sample $LiNi_{0.5}Mn_{1.5}O_4$, $LiMo_{0.05}Ni_{0.45}Mn_{1.5}O_4$ and $LiMo_{0.1}Ni_{0.45}Mn_{1.45}O_4$ at 0.5C rate.

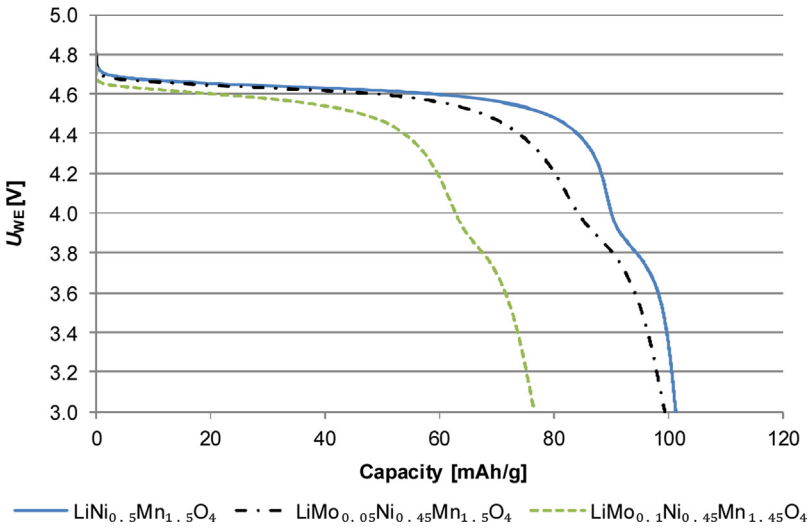

Fig. 8. Comparison of the last discharge curves of the sample $LiNi_{0.5}Mn_{1.5}O_4$, $LiMo_{0.05}Ni_{0.45}Mn_{1.5}O_4$ and $LiMo_{0.1}Ni_{0.45}Mn_{1.45}O_4$ at 2C rate.

potential of discharge plateau was lower. If we compare the potential of discharge plateau of the Mo-doped sample $LiMo_{0.05}Ni_{0.45}Mn_{1.5}O_4$ at 2C with the potential of discharge plateau of the Mo-doped sample $LiMn_{1.4}Ni_{0.55}Mo_{0.05}O_4$ referred by Yi [26] in his article we find that the sample $LiMo_{0.05}Ni_{0.45}Mn_{1.5}O_4$ presented in our article achieved almost 0.5 V higher potential than the material $LiMn_{1.4}Ni_{0.55}Mo_{0.05}O_4$.

4. Conclusions

It is clear that the used method of synthesis leads to the formation of high-voltage cathode material $LiNi_{0.5}Mn_{1.5}O_4$ and Mo doped samples. The right composition and right ratios of the elements were proved by the EDS analysis and mapping of prepared samples. Greater stability of Mo doped sample $LiMo_{0.05}Ni_{0.45}Mn_{1.5}O_4$ was demonstrated by the TGA analysis than that of the pristine sample $LiNi_{0.5}Mn_{1.5}O_4$. However, the sample $LiMo_{0.1}Ni_{0.45}Mn_{1.45}O_4$ showed worse stability during the TGA analysis. The sample $LiMo_{0.1}Ni_{0.45}Mn_{1.45}O_4$ was also less stable during cycling at various C-rates and at higher temperature which was probably caused by too high substitution of Ni and Mn by Mo. However, the sample $LiMo_{0.05}Ni_{0.45}Mn_{1.5}O_4$ showed higher capacity at lower load (0.5C) and comparable capacity with the pristine sample $LiNi_{0.5}Mn_{1.5}O_4$ at higher loads. This sample was also more stable after returning to the initial current 0.5C and during cycling at higher temperature when its capacity decreased considerably slower than in the case of the pristine sample $LiNi_{0.5}Mn_{1.5}O_4$. This improvement of electrochemical properties corresponds with better structural stability observed by the TGA analysis. Doping by a small amount of Mo therefore leads to an improvement of structural stability and particular improvements of stability during cycling at elevated temperatures. Capacity achieved by the doped sample $LiMo_{0.05}Ni_{0.45}Mn_{1.5}O_4$ is comparable with the data presented in the article by Yi [26] but unlike his article there was not observed a significant increase of capacity at higher C-rates compared with the pristine sample. However, higher potential of the discharge plateau was achieved during discharging at 2C then in the article by Yi.

Acknowledgements

This research has been carried out in the Centre for Research and Utilization of Renewable Energy (CVVOZE). Authors gratefully acknowledge the financial support from the Ministry of Education,

Youth and Sports of the Czech Republic under NPU I programme (project No. LO1210), BUT specific research programme (project No. FEKT-S-14-2293).

References

[1] H. Yoo, E. Markevich, G. Salitra, D. Sharon, D. Aurbach, On the challenge of developing advanced technologies for electrochemical energy storage and conversion, Mater. Today 17 (2014) 110–121.
[2] Y. Gao, K. Myrtle, M. Zhang, J. Reimers, J. Dahn, Valence band of LiNi x Mn 2-x, Phys. Rev. B 54 (1996) 16670–16675.
[3] J. Xu, S. Dou, H. Liu, L. Dai, Cathode materials for next generation lithium ion batteries, Nano Energy 2 (2013) 439–442.
[4] Lithium Ion Batteries – New Developments, InTech, Croatia, 2012.
[5] M. Hu, X. Pang, Z. Zhou, Recent progress in high-voltage lithium ion batteries, J. Power Sources 237 (2013) 229–242.
[6] N. Amdouni, K. Zaghib, F. Gendron, A. Mauger, C. Julien, Structure and insertion properties of disordered and ordered LiNi0.5Mn1.5O4 spinels prepared by wet chemistry, Ionics 12 (2006) 117–126.
[7] R. Brodd, Batteries for Sustainability: Selected Entries from the Encyclopedia of Sustainability Science and Technology, Springer-Verlag New York, New York, 2013.
[8] J. Xiao, X. Chen, P. Sushko, M. Sushko, L. Kovarik, J. Feng, Z. Deng, J. Zheng, G. Graff, Z. Nie, D. Choi, J. Liu, J. Zhang, M. Whittingham, High-Performance LiNi0. 5Mn1. 5O4 spinel controlled by mn3 concentration and site disorder, Adv. Mater. 24 (2017) 2109–2116 (n.d.).
[9] J. Kim, S. Myung, C. Yoon, S. Kang, Y. Sun, Comparative study of LiNi 0. 5 Mn 1. 5 o 4 − δ and LiNi 0. 5 Mn 1. 5 O 4 cathodes having two crystallographic structures: fd 3 ¯m and P 4 3 32, Chem. Mater. 16 (2004) 906–914.
[10] X. Chen, W. Xu, J. Xiao, M. Engelhard, F. Ding, D. Mei, D. Hu, J. Zhang, J. Zhang, Effects of cell positive cans and separators on the performance of high-voltage Li-ion batteries, J. Power Sources 213 (2012) 160–168.
[11] R. Santhanam, B. Rambabu, Research progress in high voltage spinel LiNi0.5Mn1.5O4 material, J. Power Sources 195 (2010) 5442–5451.
[12] O. Sha, Z. Qiao, S. Wang, Z. Tang, H. Wang, X. Zhang, Q. Xu, Improvement of cycle stability at elevated temperature and high rate for LiNi0.5-xCuxMn1.5O4 cathode material after Cu substitution, Mater. Res. Bull. 48 (2013) 1606–1611.
[13] H. Wang, T. Tan, P. Yang, M. Lai, L. Lu, High-Rate performances of the Ru-Doped spinel LiNi 0.5 Mn 1.5 O 4: effects of doping and particle size, J. Phys. Chem. C 115 (2011) 6102–6110.
[14] S. Park, W. Eom, W. Cho, H. Jang, Electrochemical properties of LiNi0.5Mn1.5O4 cathode after Cr doping, J. Power Sources 159 (2006) 679–684.
[15] G. Liu, L. Wen, G. Liu, Y. Tian, Rate capability of spinel LiCr0.1Ni0.4Mn1.5O4, J. Alloys Compd. 501 (2010) 233–235.
[16] X. Nie, B. Zhong, M. Chen, K. Yin, L. Li, H. Liu, X. Guo, Synthesis of LiCr0.2Ni0.4Mn1.4O4 with superior electrochemical performance via a two-step thermo polymerization technique, Electrochim. Acta 97 (2013) 184–191.
[17] G. Zhong, Y. Wang, Z. Zhang, C. Chen, Effects of Al substitution for Ni and Mn on the electrochemical properties of LiNi0.5Mn1.5O4, Electrochim. Acta 56 (2011) 6554–6561.
[18] G. Zhong, Y. Wang, Y. Yu, C. Chen, Electrochemical investigations of the LiNi0.45M0.10Mn1.45O4 (M = Fe, Co Cr) 5 V cathode materials for lithium ion batteries, J. Power Sources 205 (2012) 385–393.
[19] S. Oh, S. Myung, H. Kang, Y. Sun, Effects of Co doping on Li[Ni0.5CoxMn1.5-x]O4 spinel materials for 5 V lithium secondary batteries via co-precipitation, J. Power Sources 189 (2009) 752–756.
[20] J. Kim, S. Myung, C. Yoon, I. Oh, Y. Sun, Effect of ti substitution for mn on the structure of LiNi[sub 0.5]Mn[sub 1.5-x]Ti[sub x]O[sub 4] and their electrochemical properties as lithium insertion material, J. Electrochem. Soc. 151 (2004) A1911.
[21] R. Alcántara, M. Jaraba, P. Lavela, J. Tirado, E. Zhecheva, R. Stoyanova, Changes in the local structure of LiMg y Ni 0.5 − y Mn 1.5 O 4 electrode materials during lithium extraction, Chem. Mater. 16 (2004) 1573–1579.
[22] P. Wu, X. Zeng, C. Zhou, G. Gu, D. Tong, Improved electrochemical performance of LiNi0.5-xRhxMn1.5O4 cathode materials for 5 V lithium ion batteries via Rh-doping, Mater. Chem. Phys. 138 (2013) 716–723.
[23] S. Prabakar, S. Han, S. Singh, D. Lee, K. Sohn, M. Pyo, W-doped LiWxNi0.5Mn1.5-xO4 cathodes for the improvement of high rate performances in Li ion batteries, J. Power Sources 209 (2012) 57–64.
[24] T. Kazda, J. Vondrák, V. Noto, A. Fedorková, M. Sedlaříková, P. Čudek, P. Vyroubal, The influence of used precursors on the properties of high-voltage cathode materials, J. Solid State Electrochem. 19 (2014) 647–653.
[25] T. Kazda, J. Vondrák, V. Di Noto, M. Sedlaříková, P. Čudek, L. Omelka, L. Šafaříková, V. Kašpárek, Study of electrochemical properties and thermal stability of the high-voltage spinel cathode material for lithium-ion accumulators, J. Solid State Electrochem. 19 (2015) 1579–1590.
[26] T. Yi, B. Chen, Y. Zhu, X. Li, R. Zhu, Enhanced rate performance of molybdenum-doped spinel LiNi0.5Mn1.5O4 cathode materials for lithium ion battery, J. Power Sources 247 (2014) 778–785.